EDDY FLUX MEASUREMENTS OVER LAKE ONTARIO* **

S. D. SMITH

Atlantic Oceanographic Laboratory, Bedford Institute of Oceanography, Dartmouth, N.S., Canada

(Received 18 May, 1973)

Abstract. Wind, temperature and humidity fluctuations have been recorded using a sonic anemometer-thermometer, a thrust anemometer, and a Lα humidiometer. The two anemometers agree in wind speed and stress. Exchange coefficients for momentum, heat and moisture are found to agree with values measured over other bodies of water.

Notation

The following symbols will be used in this paper:

C_{10}	Wind drag coefficient at height of 10 m (Equation (4))
C_p	Specific heat of air at constant pressure
C_T	Heat flux coefficient at height of 10 m (Equation (5))
C_Q	Evaporation coefficient at height of 10 m (Equation (6))
E	Moisture flux or evaporation rate
f	Frequency (Hz)
G, G_i	Gust factors (Equations (9) and (10))
H	Sensible heat flux
L	Monin-Obukhov stability length
Q	Mean absolute humidity, or partial density of water vapour
Q_0	Saturation humidity at temperature T_W
q	Humidity fluctuation
T	Mean absolute air temperature
T_W	Water surface temperature
t	Air temperature fluctuation
t_v	Virtual air temperature fluctuation. (Virtual temperature of moist air is the temperature at which dry air would have the same density.)
U	Mean wind velocity at height z
U_{10}	Mean wind velocity at 10 m
u_i	Wind velocity fluctuation component
u	Magnitude of velocity fluctuation $(u_1^2+u_2^2+u_3^2)^{1/2}$
u_*	Friction velocity $(-\overline{u_1 u_3})^{1/2}$
V	Magnitude of wind speed
W	Indicated mean vertical wind, in anemometer coordinates

* Contribution 391, Bedford Institute of Oceanography.
** Project 75BL, International Field Year for the Great Lakes.

Boundary-Layer Meteorology **6** (1974) 235–255. *All Rights Reserved*
Copyright © 1974 by D. Reidel Publishing Company, Dordrecht-Holland

z	Height of sensor
θ	Indicated tilt of anemometer relative to mean wind
θ_h	Horizontal wind direction
ϱ	Density of air
σ_i	RMS wind fluctuation component $(\overline{u_i^2})^{1/2}$
τ	Reynolds stress or momentum flux $-\varrho\overline{u_1 u_3}$
$\phi_{ij}(f)$	Frequency spectrum or cospectrum
1, 2, 3	as subscripts refer to downwind, lateral and vertical components, respectively, in right-handed Cartesian coordinates

Overbars denote averages over a data run, which must be long enough to give statistically meaningful averages of the turbulence properties, but not so long that the wind velocity or the temperature and humidity gradients change appreciably during the run. Most data runs are of about 44-min duration.

1. Introduction

A series of eddy flux measurements have been made at a location in Lake Ontario as part of the International Field Year for the Great Lakes (IFYGL). The purpose of these measurements is to obtain values of eddy flux coefficients for use in calculating the momentum, heat, and water exchanges at the surface of Lake Ontario. We have coordinated our efforts with those of groups from Canada Centre for Inland Waters (CCIW) and Atmospheric Environment Service, Canada (AES) with the intention of comparing results. Our own experiment also set out to compare a thrust anemometer used for measurements of wind stress over the sea (Smith, 1970, 1973) with a sonic anemometer used in studies over ice floes (Banke and Smith, 1973; Thorpe *et al.*, 1973). The results from the Bedford Institute of Oceanography (BIO) to be presented here are the first from the three groups to become available, and comparisons with the other results will be reported at a later date.

2. Eddy Correlation Method

The fluxes of momentum, heat and water vapour are determined by obtaining mean products of the vertical velocity with the downwind velocity, temperature and humidity,

$$\tau = -\varrho\overline{u_1 u_3} \tag{1}$$

$$H = \varrho C_p \overline{t u_3} \tag{2}$$

$$E = \overline{q u_3} \tag{3}$$

at a fixed point above the surface. We assume that these fluxes are constant in the layer between the surface and the height of measurement (5 to 10 m in the present study). We shall represent the measured fluxes in terms of bulk aerodynamic coefficients

$$C_{10} = \tau/\varrho U_{10}^2 = -\overline{u_1 u_3}/U_{10}^2 \tag{4}$$

$$C_T = H/\varrho C_p U_{10}(T_W - T_{10}) = \overline{tu_3}/U_{10}(T_W - T_{10}) \tag{5}$$

$$C_Q = E/U_{10}(Q_0 - Q_{10}) = \overline{qu_3}/U_{10}(Q_0 - Q_{10}) \tag{6}$$

which allow the fluxes to be estimated from measurements of mean wind, temperature and humidity.

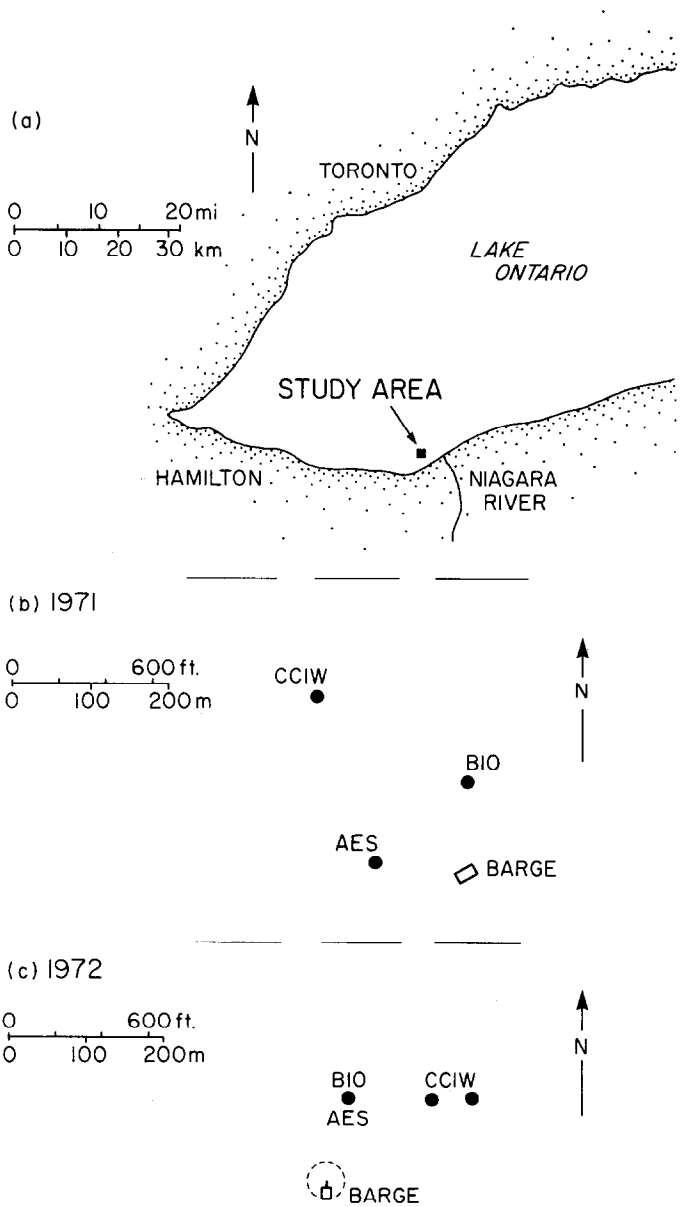

Fig. 1. Location of the instrument masts and barge: (a) position in Lake Ontario, (b) 1971, (c) 1972.

3. Experiments

Three masts were supported with guy wires in 10 m of water at Niagara Bar (43°17′ N, 70°07′ W) in the western end of Lake Ontario. Cables connected sensors on the masts to recording apparatus on a barge, moored approximately 100 m from the mast to which our sensors were attached (Figure 1). In 1971 one mast was assigned to BIO, one to AES, and one to CCIW (Figure 1b). In 1972 one mast was used by BIO and by AES at different seasons of the year, and the barge was anchored by the bow with the stern free to swing in a circle (Figure 1c). This location, 2.6 km from the nearest shore, was chosen for easy access from shore and for good exposure to winds from the north and east. We avoided recording data during periods of offshore winds from the south and west, because during these periods the boundary layer would be in a state of transition and the barge and mast would interfere with the air flow around the sensors.

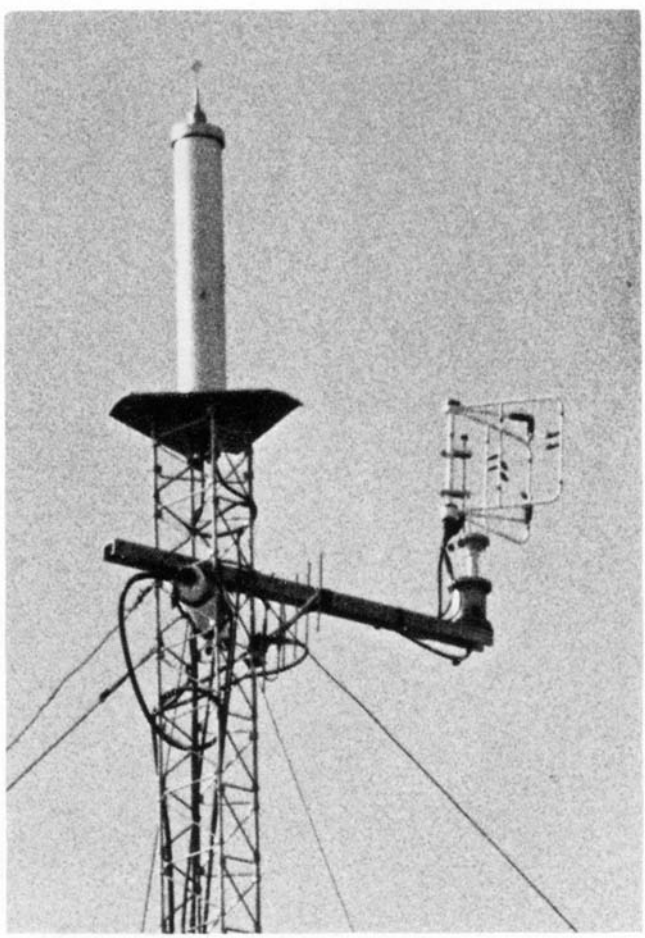

Fig. 2. Thrust anemometer (left) and sonic anemometer (right) mounted on mast.

3.1. Thrust anemometer

The Mk.VI thrust anemometer (Smith, 1969, 1970) senses the wind thrust vector on a sphere, a perforated table tennis ball of 3.8-cm diam by means of a three-component spring linkage and three differential transformers. The linkage and transformers are in a case filled with constant-viscosity silicone fluid which damps vibrations and protects the mechanism from weathering and corrosion in the marine atmosphere. The spring linkage is under-damped and has a resonant frequency at about 40 Hz. The anemometer stand used in the field incorporates an electrically-driven cover which allows the anemometer to protrude at the top when it is in operation (Figure 2) but telescopes upward to cover the anemometer and to permit recording of the signal levels at zero wind speed.

The thrust anemometer was calibrated in a wind tunnel before and after each field trip (Smith, 1969). The calibrations were recorded on analogue magnetic tape in the same format as the field data. A computer was programmed to digitize the data and calculate calibration coefficients. The anemometer stand used in the wind tunnel was of the same shape and size as that used in the field. Wind-tunnel blockage of the flow by the anemometer and stand was allowed for in the calibration.

The sensitivity of the thrust anemometer to wind force (velocity squared) is proportional to air density, so that the computed Reynolds stress given as $-\varrho\overline{u_1 u_3}$ in earlier publications is more properly expressed as $-\overline{\varrho u_1 u_3}$. Since the calibration factors have not been adjusted for changes in ϱ (up to $\pm 2\%$), the velocity sensitivity may be off by $\pm 1\%$. The measured drag coefficient and other dimensionless velocity parameters are not affected by changes in ϱ.

3.2. Sonic anemometer

The Kaijo Denki PAT 311-1 sonic three-component anemometer-thermometer is used by a number of groups to study boundary-layer turbulence. Aspects of its performance are discussed by Kaimal (1968, 1969) and Kaimal *et al.* (1968). The high wave-number response is limited by averaging over the 20-cm sound paths of the probe, but is adequate to measure spectra, cospectra and stress up to a frequency of 10 Hz in the 5 to 10 m s^{-1} wind speed range and 5 to 10 m height range which we shall be studying.

The sonic anemometer was calibrated before and after each field trip using either a wind tunnel or an electronic timer. Its sensitivity was found to remain within the manufacturer's $\pm 3\%$ tolerance. Its advantages over the thrust anemometer are linear response and a more stable zero-wind signal, while its disadvantages are complexity, higher power consumption, and a need for more frequent adjustment. The velocity sensitivity of the sonic anemometer is inversely proportional to the speed of sound and so directly proportional to the square root of air density. The Reynolds stress $-\varrho\overline{u_1 u_3}$ is of second order in velocity and is once again more properly expressed as $-\overline{\varrho u_1 u_3}$.

The sonic thermometer measures virtual temperature,

$$t_v = t + 0.47 \times 10^{-3}\, T^2 q/273$$

(Pond *et al.*, 1971) and the heat flux has been corrected by using

$$\overline{tu_3} = \overline{t_v u_3} - 0.47 \times 10^{-3}\, T^2 \overline{qu_3}/273 \tag{7}$$

where the temperature is in degrees Celsius and the humidity in gm m^{-3}. For the September 1971 data, $\overline{qu_3}$ was estimated using $C_Q = 1.4 \times 10^{-3}$. The right-hand term in Equation (7) reduces the mean value of C_T by some 12%. The atmospheric stability,

$$\frac{z}{L} = -\frac{gKz\,\overline{t_v u_3}}{T u_*^3}$$

on the other hand, was calculated using the virtual temperature and so includes the effects of both temperature and humidity.

3.3. Lα HUMIDOMETER

The Electromagnetic Research Corporation Model BLR humidiometer measures absorption of monochromatic ultraviolet radiation by water vapour in the air over a short path (about 1 to 4 cm). In our experiments the sensor was mounted 25 cm behind and 35 cm to one side of the sonic vertical wind sensor, exposed directly to the air flow without any shield or aspirator. In this configuration its frequency response was more than adequate for the 0 to 10 Hz band to be discussed here. Bottled dry air was blown into a hollow sponge placed over the sensor to obtain a zero-humidity signal. The calibration of the humidiometer was determined for each series of runs from its response to dry air and to the mean humidity of the ambient air.

3.4. DATA RECORDING AND ANALYSIS

The signals were transmitted by underwater cables from the mast to the barge, where they were frequency-modulated and recorded in frequency-multiplexed form on one track of a General Radio Model 1525 magnetic tape recorder. At the beginning of each data run, reference voltages and zero wind and humidity signals were recorded.

The data were later played back through phase-matched, linear phase shift, low-pass filters (3 db down at 11 Hz, 18 db per octave roll-off) and digitized at a rate of 20 samples per second. Computer program ATOD (Smith and Brown, 1971) was used to convert the data into the desired units using calibration factors and the reference and zero-level recordings. This program also converted the thrust anemometer signals into velocity components, linearized the humidiometer signal, removed linear trends from the data, rotated the thrust and sonic anemometer coordinates to align component 1 with the indicated mean wind, wrote the data on digital magnetic tape, and printed a data summary. The tilt of the mean wind relative to the anemometers was found to range from 0.8 to 5.4 deg (Tables I and II). This apparent updraft may have been caused by supporting the anemometers from beneath, and was removed by the coordinate rotation.

The data were fast-Fourier transformed in sequential 3.4-min (4096-sample) blocks, and spectra were computed at about eight logarithmically-spaced frequency bands per decade and averaged over about 12 blocks per run.

TABLE I

Sonic anemometer data, 1971

Run 1971	Start time GMT	Date Sept. (Oct.)	Duration min	Mean wind U_{10} m s^{-1}	Tilt θ deg	$\overline{u_1 u_3}$ (m s^{-1})^2	σ_3/u_*	K.E. flux $\frac{\overline{u^2 u_3}}{\overline{2Uu_*}^2}$	Gust factors G	G_1	G_2	G_3	Drag coefficient $10^3 C_{10}$
3	1443	26	44	5.85	4.5	−0.041	1.55	0.090	1.34	–	–	–	1.20
4	1558	26	44	5.71	3.0	−0.038	1.64	0.064	1.38	0.72	0.77	0.52	1.18
5	1656	26	44	5.30	3.0	−0.036	1.59	0.063	1.37	0.82	0.94	0.52	1.29
6	1759	26	44	5.47	2.8	−0.044	1.40	0.062	–	–	–	–	1.46
7	1757	27	44	5.83	2.2	−0.041	1.19	0.065	1.25	–	–	0.38	1.19
8	1944	27	44	7.38	2.3	−0.066	1.17	0.052	1.22	–	–	0.36	1.22
9	2051	27	43	7.68	3.1	−0.074	1.20	0.053	1.24	–	–	0.42	1.26
11	1632	30	44	4.60	0.8	−0.018	1.32	0.051	1.34	0.73	0.66	0.45	0.87
12	1732	30	44	5.09	1.2	−0.022	1.26	0.047	1.26	–	–	0.43	0.85
13	1920	30	43	5.29	1.4	−0.023	1.25	0.069	1.30	0.65	0.66	0.39	0.82
14	2129	(3)	31	8.80	1.6	−0.079	1.16	0.020	1.30	0.64	0.53	0.40	1.03
15	2216	(3)	38	8.17	1.6	−0.056	1.15	0.038	1.24	0.56	0.55	0.36	0.84
17	1908	(8)	40	7.16	1.7	−0.053	1.29	0.054	1.46	1.04	1.09	0.56	1.03
18	2013	(8)	39	7.96	1.5	−0.076	1.11	0.002	1.43	1.03	0.79	–	1.19
19	1403	(13)	23	5.11	3.2	−0.030	1.31	0.007	–	–	–	0.49	1.14
20	2000	(13)	25	8.02	1.0	−0.062	1.15	0.058	1.25	0.62	0.78	0.34	0.96
21	2100	(13)	41	8.20	1.5	−0.066	1.17	0.029	1.30	0.68	0.62	0.37	0.98
22	1437	(14)	42	7.09	1.6	−0.050	1.22	0.004	–	–	–	0.39	1.00
23	1548	(14)	26	7.72	2.2	−0.063	1.21	0.016	1.39	0.73	0.69	0.51	1.05
Mean							1.28		1.32	0.75	0.73	0.43	1.08
Standard deviation							0.16		0.07	0.16	0.17	0.07	0.18

Note: Runs 2 to 9 at 10-m height, runs 11 to 23 at 5.2-m height.

TABLE II

Thrust and sonic anemometer data, 1972

Run 1972	Start time GMT	Date June	Duration min	Mean wind U_{10} m s^{-1}	Tilt θ deg	$\overline{u_1 u_3}$ (m s^{-1})^2	σ_3/u_*	K.E. flux $\frac{\overline{u^2 u_3}}{2Uu_*^2}$	Gust factors G	G_1	G_2	G_3	Drag coefficient $10^3 C_{10}$
3S	2158	16	44	3.76	3.2	−0.010	1.29	0.003	–	–	–	–	0.68
4T	1653	17	44	7.60	0.9	−0.071	1.08	0.052	1.22	0.50	0.49	0.34	1.23
4S				7.80	3.6	−0.085	1.18	0.059	1.20	0.47	0.50	0.44	1.39
5T	1850	17	44	4.86	3.8	−0.034	1.05	0.032	1.26	0.56	0.52	0.41	1.44
5S				5.11	4.4	−0.038	1.11	0.037	1.28	0.58	0.50	0.46	1.45
6T[a]	1955	17	26	3.94	2.4	−0.006	2.04	0.089	1.20	0.51	0.41	0.37	0.41
6S				4.08	3.1	−0.012	1.41	0.066	1.19	0.46	0.46	0.36	0.72
7T	1637	18	44	9.09	5.4	−0.097	1.18	0.019	1.28	0.62	0.47	0.43	1.18
7S				9.26	3.9	−0.097	1.38	0.028	1.28	0.62	0.54	0.48	1.13
8T	1738	18	44	10.16	3.9	−0.119	1.18	0.011	1.29	0.56	0.52	–	1.15
8S				9.99	4.1	−0.110	1.49	0.027	1.31	0.61	0.56	0.46	1.10
9T	1836	18	44	9.54	3.9	−0.115	1.17	0.004	1.29	0.56	0.46	0.41	1.26
9S				9.49	4.0	−0.104	1.42	0.015	1.28	0.58	0.50	0.46	1.16
10T	1937	18	44	9.09	2.6	−0.088	1.26	0.010	1.30	0.62	0.45	–	1.07
10S				9.02	3.6	−0.096	1.38	0.019	–	–	–	–	1.18
11T	2035	18	40	9.08	1.9	−0.090	1.33	0.012	1.28	0.58	0.48	0.56	1.09
11S				9.26	3.8	−0.105	1.41	0.012	1.30	0.58	0.52	0.53	1.22
12T[a]	1920	19	44	4.45	4.4	−0.019	1.18	0.008	1.22	0.49	0.46	0.34	0.94
12S				4.60	2.7	−0.015	1.39	0.071	1.23	0.45	0.46	0.36	0.70
13S	1630	21	40	3.47	3.2	−0.006	1.33	0.019	1.21	0.45	0.46	0.31	0.48
14S	1820	21	26	3.04	4.0	−0.009	1.16	0.068	1.26	0.64	0.60	0.36	0.98
15S	1921	21	44	7.50	3.5	−0.067	1.41	0.022	1.42	0.75	0.74	0.52	1.19
Mean T							1.18		1.27	0.57	0.48	0.43	1.20
Standard deviation							0.10		0.03	0.04	0.03	0.08	0.13
Mean S							1.32		1.27	0.56	0.53	0.43	1.03
Standard deviation							0.12		0.06	0.10	0.08	0.07	0.30

Note: T – Thrust anemometer, height 9.6 m. S – Sonic anemometer, height 8.9 m.

[a] Not used in computing means and standard deviations.

4. Results

4.1. Comparison between sonic and thrust anemometers

The anemometer comparison is based on simultaneous runs 4 to 12 (Table II) on 17 to 19 June 1972. The thrust anemometer was also operated during the 1971 experiments but a translucent cover was used which was later found when closed to warm the thrust anemometer by 10 to 15 °C by a greenhouse effect on sunny days. The vertical component of the thrust anemometer drifted with temperature variations when the cover was opened and reasonable results were obtained only on a few occasions with heavy overcast skies. This problem was overcome by coating the thrust anemometer cover with reflecting metallic tape, reducing the greenhouse effect to less than 0.5 °C.

The results from the thrust and sonic anemometers agreed well at wind speeds above 5 m s^{-1}. Taking the sonic anemometer to be correct, the mean and rms discrepancies in U_{10} from the thrust anemometer (Table III) were 0.1%, and 2%, respectively., The

TABLE III

Thrust anemometer error, relative to sonic anemometer

Run 1972	Sonic U_{10} m s^{-1}	U_{10} % error	C_{10} % error	σ_1/U % error	σ_2/U % error	σ_3/U % error
4	7.8	−2.6	−12	0	−5	−14
5	5.1	−4.5	− 1	6	−3	− 7
6	4.1[a]	−3.4	−43	6	−7	− 7
7	9.3	−1.9	5	2	−2	−13
8	10.0	1.9	4	−3	−3	−18
9	9.5	0.1	10	1	−5	−13
10	8.8	2.9	−10	1	−4	−12
11	9.2	−1.7	−11	1	0	2
12	4.6[a]	−3.3	34	6	4	− 3
Mean		0.1	− 2	1	−3	−11
Std. Dev.		2.6	8			

[a] Thrust anemometer data not reliable for $U_{10} < 5$ m s^{-1}. These runs were not used in calculating means and standard deviations.

mean and rms discrepancies in C_{10} were −2% and 8%, respectively. At lower wind speeds, the discrepancies became much larger since the signal levels from the thrust anemometer became too low for accurate stress measurements. For runs 6 and 12, at about 4 m s^{-1}, the thrust anemometer drag coefficients differed by −43 and 34%, respectively.

The downwind spectra for a typical run, 1972-9, (Figure 3a) agree closely at all analyzed frequencies, showing that both anemometers have very similar responses over the frequencies analyzed (0.004 to 10 Hz). The stress cospectrum $\phi_{13}(f)$ (Figure 4) shows similarly good agreement. Both anemometers show negative quadrature spectra from 0.05 to 0.5 Hz as observed by Smith (1970). The spectra and cospectra contain no sharp peaks at the wave frequency (about 0.3 Hz).

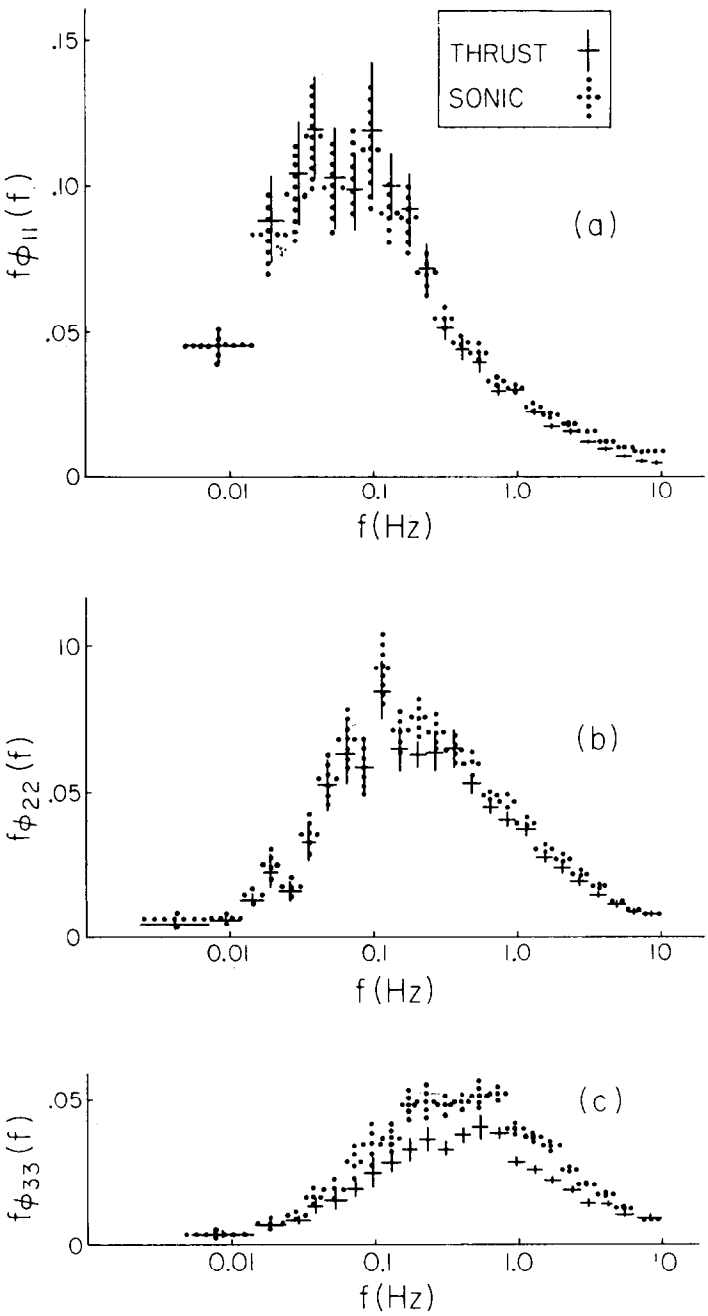

Fig. 3. Spectra of wind turbulence for Run 1972-9: (a) downwind, (b) lateral, and (c) vertical. Width of symbols gives bandwidth and height gives standard error among the analyzed blocks.

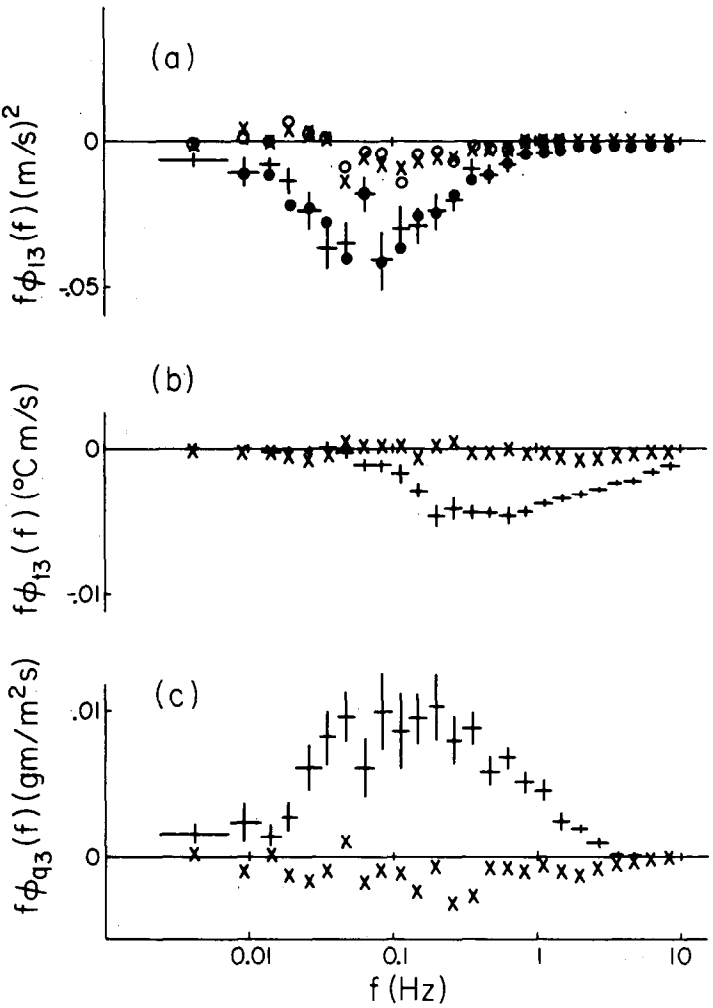

Fig. 4. Cospectra for Run 1972-9. (a) Thrust anemometer wind stress cospectrum $f\phi_{13}(f)$ (●) and quadrature spectrum $f\phi_{13}^*(f)$ (○); sonic anemometer $f\phi_{13}(f)$ (+) and $f\phi_{13}^*(f)$ (×). (b) Sonic anemometer-thermometer heat flux cospectrum $f\phi_{t_3}(f)$ (+) and quadrature spectrum (×); (c) Evaporation spectrum $f\phi_{q_3}(f)$ (+) and quadrature spectrum $f\phi_{q_3}^*(f)$ (×). Positive quadrature spectrum is for u_3 lagging in each case.

In spite of good agreement in the downwind component and drag coefficient (Table III), the thrust anemometer was 3% less sensitive to lateral wind fluctuations than the sonic anemometer and 11% less sensitive to vertical winds. These calibration discrepancies are also seen in the lateral and vertical spectra (Figures 3b and 3c), although the shapes of the spectra are the same. The ratio σ_3/u_* is lower for the thrust anemometer than for the sonic anemometer in each of the comparison runs. The mean value of this ratio for the thrust anemometer measurements is 1.2 ± 0.1 (standard deviation), and for the 32 sonic anemometer measurements, 1.3 ± 0.1. The value of this

ratio is generally found to average between 1.2 and 1.4 in neutral boundary-layer turbulence at heights from 3 to 15 m (1.3, Pond *et al.*, 1971; 1.4, McBean, 1971; 1.2, Smith, 1972; 1.2, Banke and Smith, 1973; 1.3, Smith, 1973) and so neither of the present values is without precedent.

At frequencies below 0.3 Hz, all three velocity components are highly coherent (>0.9) and in phase within 10 deg (Figure 5), and so both anemometers are reproducing the same wind fluctuations. The vertical coherence is slightly smaller because of the lower spectral levels (Figure 3) and lower signal to noise ratios. At frequencies between 0.3 Hz and 3 Hz, the observed phase characteristics can be explained by the sonic anemometer being located approximately 0.8 m upwind of and 0.7 m below the thrust anemometer. According to the Taylor or 'frozen turbulence' hypothesis, the thrust

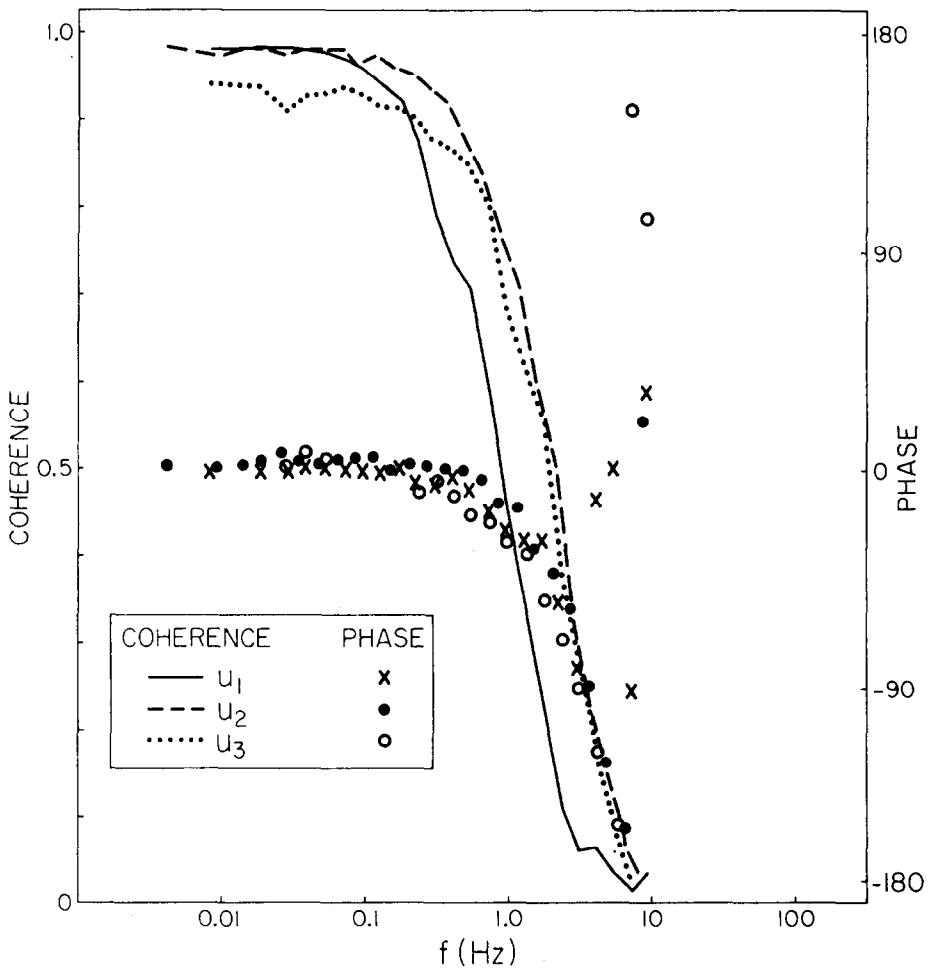

Fig. 5. Coherence and phase spectra for Run 1972-9. Positive phase corresponds to thrust anemometer leading. Sonic anemometer was approximately 0.8 m upwind of thrust anemometer, causing a phase shift of $-90°$ at approximately 3 Hz.

anemometer signals should lag the sonic anemometer signals by 360 deg at a separation of one wavelength, corresponding to a frequency of $U/0.8 \simeq 12$ Hz, and we should look for a phase shift of $-30°$/Hz in the thrust anemometer signal. The measured phases are close to $-90°$ at 3 Hz. Above this frequency, the downwind phases become scattered, while the phases of the lateral and vertical components continue to shift but at a slightly lower rate. The coherence also falls off rapidly with increasing frequency, passing through 0.5 at 1 Hz (wavelength 9 m) for the downwind component and 3 Hz (wavelength 3 m) for the lateral and vertical components. The earlier loss of coherence by the downwind component has been observed by Smith (1972) to be characteristic of boundary-layer turbulence at a number of lateral separations, and the downwind and lateral half-coherence wavelengths were found to be quite similar (at 1.2-m lateral separation) to the present results at 1.1-m downwind and vertical separation.

At frequencies above 3 Hz, the low coherence precludes further detailed comparison. The thrust anemometer components have mechanical resonances at about 40 Hz which may introduce phase shifts of $\pm 180°/40$ Hz $= \pm 4.5°$/Hz, but these phase shifts are too small to resolve. Frequencies above 3 Hz are relatively unimportant in flux measurements and so phase shifts of up to $\pm 45°$ at 10 Hz are acceptable.

4.2. Drag coefficient

The average drag coefficient from all the measurements (Tables I and II) is $10^3 C_{10} = 1.08 \pm 0.22$ (standard deviation). A regression line of C_{10} on U_{10} (Figure 6)

$$10^3 C_{10} = (0.82 + 0.039\, U_{10}) \pm 0.20 \tag{8}$$

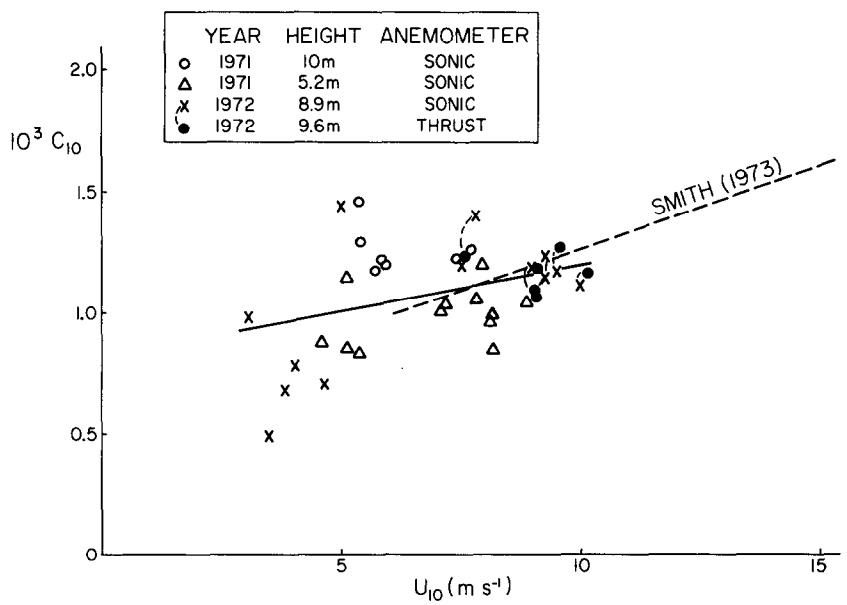

Fig. 6. The drag coefficients as a function of wind speed. Regression line, solid; regression line from Smith (1973), dashed. Dotted lines join simultaneous measurements.

with a correlation coefficient of 0.36 indicates a smaller variation with wind speed than that over the Atlantic Ocean reported by Smith (1973), $10^3 C_{10} = (0.58 + 0.068 U_{10}) \pm 0.24$. This larger variation may be attributable to the longer fetch and higher sea states.

A Students t test indicates that $t = 2.34$ with 37 deg of freedom (39 drag coefficients) and that the variation of drag coefficient in the present data is significant at the 3% level, i.e., probably real from a statistical point of view, although the regression line does not fit the data a great deal better than does a constant C_{10}.

Regression lines fitted to drag coefficients from a number of recent studies (Hasse, 1968; Brocks and Krügermeyer, 1970; Miyake *et al.*, 1970; Sheppard *et al.*, 1972) give values of $10^3 C_{10} = 1.2$ to 1.4 at a wind speed of 10 m s^{-1}. Smith (1973) found $10^3 C_{10} = 1.26$ at 10 m s^{-1}, and noted slightly lower drag coefficients in limited-fetch situations corresponding more closely to those at the present site.

For calculating the stress field over the lake from observed surface winds, the value at a wind speed of 10 m s^{-1}, $10^3 C_{10} = 1.2$ may be used. Since the stress at lower wind speeds is relatively small, a slight overestimate in these cases would not be important. Much higher wind speeds occur only infrequently. An alternative method of determining a drag coefficient which puts more weight on the higher wind speed cases is the fitting of a regression line of $\overline{u_1 u_3}$ on U_{10}^2 for 39 runs from Tables I and II,

$$\overline{u_1 u_3} = -0.002 (m\,s^{-1})^2 + 1.2 \times 10^{-3}\ U_{10}^2 \pm 0.007\ (m\,s^{-1})^2;$$ correlation coefficient 0.98.

The slope of this regression line again gives $C_{10} = 1.2 \times 10^{-3}$.

4.3. Turbulence levels

The turbulence levels (Table IV) are in reasonably good agreement with those from Smith (1973) over the Atlantic Ocean and from other similar studies. The lower vertical sensitivity of the thrust anemometer is not evident in Table III because thrust anemometer data were not obtained for several runs (3, 12, 13, 14 in 1972) at low wind speeds and low vertical turbulence levels.

TABLE IV

Turbulence levels

Anemometer	Year	No. of runs		σ_1/U	σ_2/U	σ_3/U
Sonic	1971	19	Mean	0.097	0.093	0.044
			Std. dev.	0.018	0.030	0.007
Thrust	1972	6	Mean	0.078	0.057	0.043
			Std. dev.	0.004	0.002	0.004
Sonic	1972	13	Mean	0.079	0.066	0.042
			Std. dev.	0.011	0.012	0.009
Thrust[a]	1968–9	39	Mean	0.081	0.067	0.045
			Std. dev.	0.009	0.014	0.006

[a] Atlantic Ocean data from Smith (1973).

4.4. Gust factors

In applications such as the design of structures, the peak velocity is of greater importance than the mean wind. A gust factor which is the ratio of the peak downwind

velocity to the mean,

$$G = 1 + (u_{1\,\max}/U) \tag{9}$$

is listed in Tables I and II. The mean value is $G = 1.30 \pm 0.08$. Smith (1973) reports a similar value, 1.29 ± 0.04, over the Atlantic Ocean, and Wieringa (1973) gives $G = 1.25$ for one-second averages in 10-min runs at 8 m above a lake.

The range of variation of each wind component,

$$G_i = (u_{i\,\max} - u_{i\,\min})/U \tag{10}$$

is also listed in Tables I and II. The mean vertical gust factor $G_3 = 0.43 \pm 0.07$ gives the range of wind tilt in radians, which amounts to $\pm 12°$, again in close agreement with Smith (1973). A similar interpretation of G_2 as the range of wind azimuth varia-

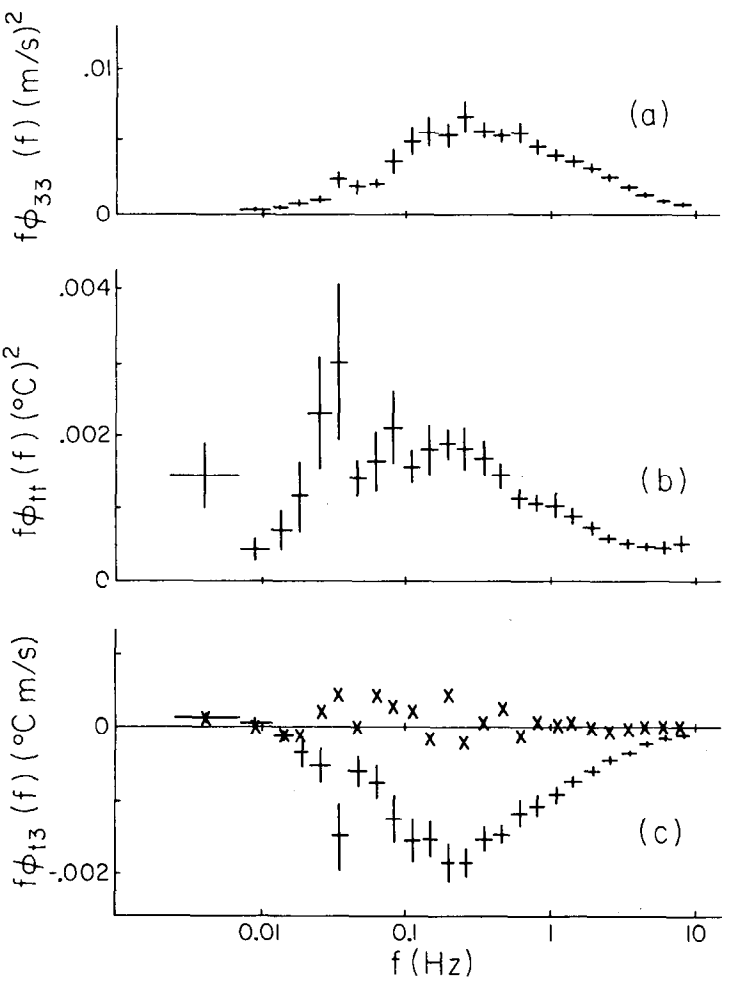

Fig. 7. Spectra of (a) vertical wind, (b) temperature, and (c) heat flux cospectrum (+) and quadrature spectrum (×) for Run 1972-3.

TABLE V

Heat and water vapour fluxes

Run	Start time GMT		ΔT_{10} °C	ΔQ_{10} g m^{-3}	Relative humidity %	Sonic thermometer σ_{tv} °C	$\overline{tu_3}$ °C m s^{-1}	z/L	$10^3 C_T$	Lα humidiometer σ_q gm m^{-3}	qu_3 gm m^{-2} s^{-1}	$10^3 C_Q$
1971		Sept.										
3	1443	26	3.0	4.8	80	0.21	0.024	−0.04	1.4			
4	1558	26	2.9	4.5	79	0.22	0.021	−0.06	1.9			
5	1656	26	2.4	4.3	78	0.21	0.028	−0.05	2.2			
6	1759	26	2.4	4.3	78	0.19	0.024	−0.04	1.8			
7	1757	27	1.9	3.5	84	0.12	0.010	−0.02	0.9			
8	1944	27	1.5	3.1	89	0.14	0.015	−0.01	1.4			
9	2051	27	1.9	2.6	89	0.15	0.012	−0.01	0.8			
11	1632	30	2.2	3.8	83	0.12	0.007	−0.05	0.7	0.32	0.024	1.4
12	1732	30	1.9	3.8	83	0.14	0.007	−0.04	0.7	0.30	0.028	1.5
13	1920	30	1.6	3.6	84	0.14	0.008	−0.04	1.0			
		Oct.										
14	2129	3	0.6	2.5	90	0.15	0.005	−0.01				
15	2216	3	0.2	2.5	90	0.13	0.004	−0.01				
17	1908	8	−0.1	4.0	66	0.15	0.007	0.00				
18	2013	8	−1.3	4.0	66	0.14	0.002	−0.02				
19	1403	13	0.2	4.0	68	0.12	0.006	0.01				
20	2000	13	0.0	2.7	79	0.15	0.007	0.00				
21	2100	13	0.2	3.6	77	0.10	−0.002	0.01				
22	1437	14	−1.8	1.6	81	0.09	−0.012	0.00				
23	1548	14	0.9	1.5	84	0.07	−0.007	0.00				
1972		June										
3S	2158	16	−1.8	4.3	60	0.14	−0.007	0.93	1.0			
4S	1653	17	1.9	5.7	67	0.20	0.025	−0.13	1.7			
5S	1850	17	−0.5	6.8	52	0.05	0.001	−0.02	[a]	0.49	0.056	1.6
6S	1955	17	0.0	6.4	56	0.07	0.000	−0.01	[a]	0.34	0.020	0.8
7S	1637	18	−0.1	4.2	71					0.25	0.039	1.0
8S	1738	18	−0.1	3.8	74	0.10	−0.008	0.02	[a]	0.22	0.042	1.1
9S	1836	18	−0.5	3.5	74	0.10	−0.014	0.04	[a]	0.21	0.038	1.2
10S	1937	18	−0.1	3.8	74	0.10	−0.016	0.07	[a]	0.18	0.031	0.9
11S	2035	18	−0.5	4.2	70	0.08	−0.013	0.05	[a]	0.24	0.045	1.2
13S	1630	21	−0.7	−0.3	98	0.32	−0.003	0.09	1.2			
15S	1921	21	−0.2	1.3	89	0.15	−0.018	0.13	[a]			

[a] ΔT too small for reliable determination of C_T.

tion must be applied with caution, since we have avoided analysis of data recorded during periods of rapidly changing wind direction. Because the lateral and vertical velocities were always substantially smaller than the downwind velocity, a gust factor computed using the maximum absolute value of the velocity would not differ appreciably from G. In a few cases, flaws in the recording caused 'spikes' and the gust factors had to be omitted from Tables I and II.

4.5. Heat flux

In nearly neutral stratification the temperature fluctuations were small and the high-frequency end of the temperature spectrum (not shown) and heat-flux cospectrum (Figure 4b) were affected by system noise at frequencies above 1 Hz. The temperature spectrum for Run 1972-3 (Figure 7) was noisy only at frequencies above about 3 Hz. The heat-flux cospectrum was less susceptible to noise than the temperature spectrum; in other words, the noise in the temperature signal was not highly correlated with the vertical wind (Figure 7a). Examination of the heat-flux cospectrum (Figure 7c) indicates that the measured heat flux did not have significant contribution at frequencies above 3 Hz and that the measured heat flux was not significantly affected by high-frequency noise in the recorded temperature signal. A similar examination of all the

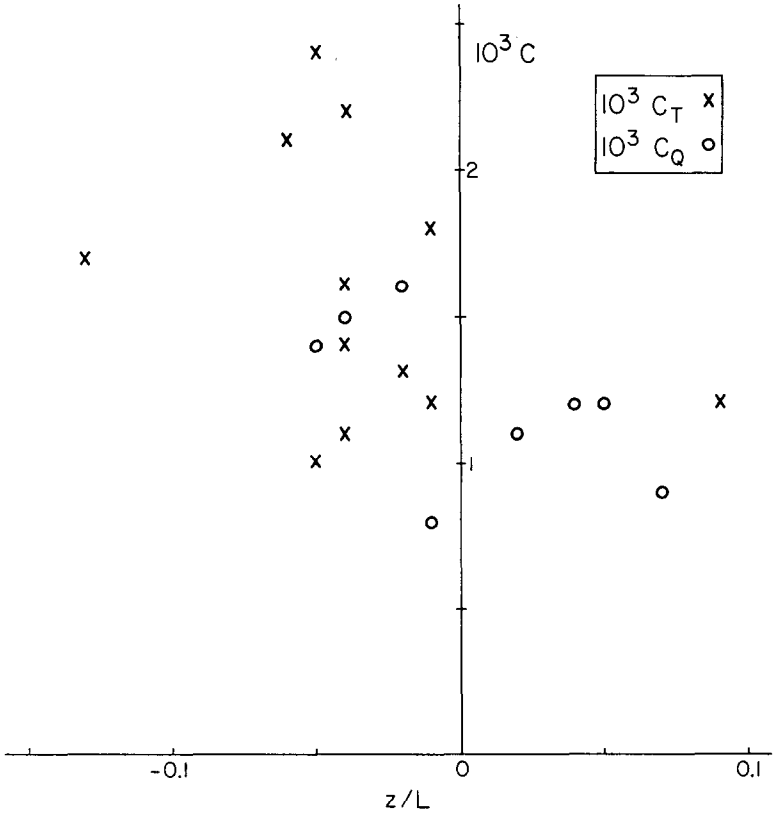

Fig. 8. Heat flux (×) and evaporation coefficients (○) as a function of stability.

temperature spectra and heat-flux cospectra showed that values of $\overline{tu_3}$ could be used to find C_T (Table V) on most occasions when the magnitude of the water-air temperature difference exceeded 0.5 °C. These had a mean value $10^3 C_T = 1.3 \pm 0.5$ (standard deviation). For the same 13 runs, a regression line

$$\overline{tu_3} = -3 \times 10^{-4}\,^{\circ}\mathrm{C\,m\,s^{-1}} + 1.3 \times 10^{-3}(T_W - T_{10}) \pm 1.3 \times 10^{-3}\,^{\circ}\mathrm{C\,m\,s^{-1}};$$

correlation coefficient 0.86

again gives a slope $C_T = 1.3 \times 10^{-3}$. The humidity correction term in Equation (11) amounted to a large fraction of the measured heat flux (over 100% in one case) in October 1971 and C_T is not listed in these cases. The heat flux coefficients (Figure 8) obtained in stable conditions have below-average values, and the most unstable runs yield above-average values. Most of the results pertain to slightly unstable stratification and do not help us to establish the size of a trend for C_T with stability. Other

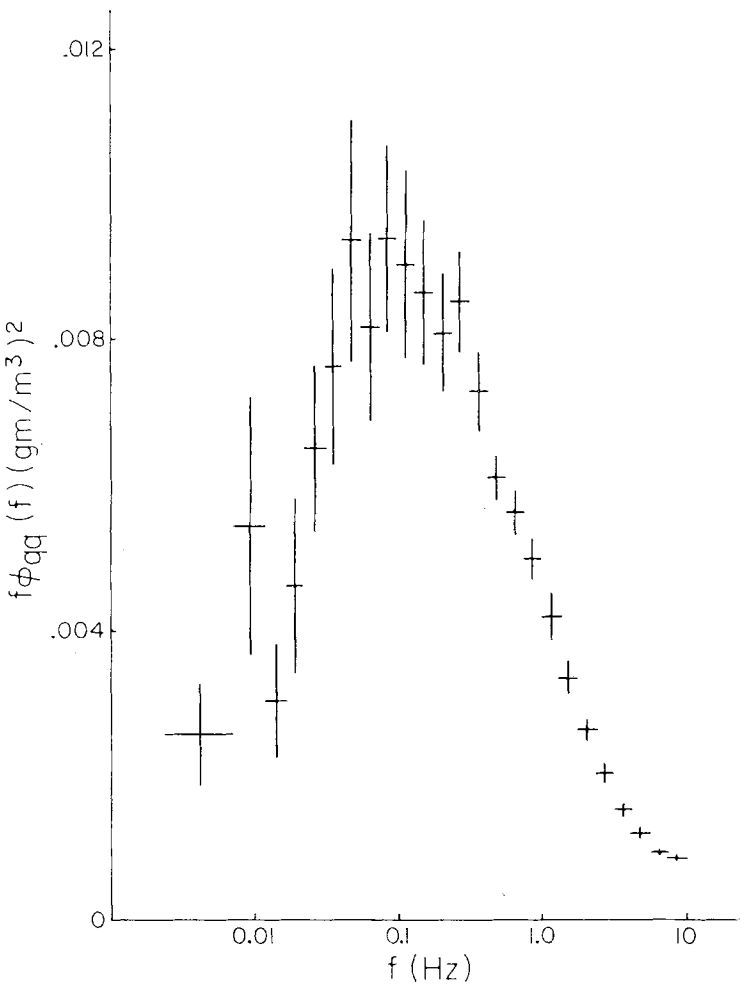

Fig. 9. The humidity spectrum for Run 1972-9.

IFYGL boundary-layer studies in the winter and summer seasons will cover a wider range of stability. Hasse (1968) gives a slightly lower value, $C_T = 1 \times 10^{-3}$.

4.6. Evaporation

The humidity spectrum (Figure 9) peaked at a frequency between the peaks of the downwind and temperature spectra. No problems with noise were encountered, but the humidity sensor could not be operated without damage during periods of precipitation or very high humidity. The cospectrum of evaporation (Figure 4c) peaks at a slightly higher frequency than that of wind stress, but the heat-flux cospectrum peaks at a higher frequency again. Miyake *et al.* (1970) noted that heat-flux cospectra over land in slightly unstable stratification were flatter and extended to higher frequencies than the evaporation and momentum flux cospectra. Pond *et al.* (1971), Figures 3 and 4, showed evaporation cospectra peaking at a frequency between the peaks of the momentum and heat-flux cospectra. The evaporation coefficients (Table V), measured during nine runs, have a mean value $10^3 C_Q = 1.2 \pm 0.3$. A regression line for the same 9 runs,

$$\overline{qu_3} = 0.005 \text{ g m}^2 \text{ s}^{-1} + 1.0 \times 10^{-3}\, U_{10}(Q_0 - Q_{10}) \pm 0.7 \text{ g m}^2 \text{ s}^{-1};$$
correlation coefficient 0.72

has a slope $C_Q = 1.0 \times 10^{-3}$. This places more weight on the cases with greater evaporation. In view of the scatter in the data, the difference between the two values for C_Q is not highly significant, and all three eddy flux coefficients may be taken to be the same,

$$C_{10} = C_T = C_Q = 1.2 \times 10^{-3}.$$

Pond *et al.* (1971) give a similar value, $10^3 C_Q = 1.2 \pm 0.2$ from measurements at a floating platform. The three most unstable runs have higher evaporation coefficients than the remaining runs (Figure 8), but once again the small range of stability and the scatter in the data prevent us from determining the amount of variation with stability.

4.7. Vertical flux of kinetic energy

The mean vertical kinetic energy flux expressed as a fraction of the downward mean-wind energy flux $\overline{u_3 u^2}/2Uu_*^2$ (Tables I and II, Figure 10) increases with increasing instability for negative z/L and is small for positive z/L, but does not follow the relations established over ice in the Gulf of St. Lawrence (Smith, 1973) or in the Arctic (Banke and Smith, 1973). The flux is upwards in all cases, although at much lesser heights we might expect to find a downward flux of energy into the surface waves.

The vertical gradient of the kinetic energy flux contributes to the turbulent kinetic energy budget. The present measurements were made at about twice the elevation of the measurements over ice. We find about twice as much variation with stability in the present results, indicating that the vertical kinetic energy flux may be approximately proportional to height. The agreement between the thrust and sonic anemometers is not as good as it was for wind stress; the sonic anemometer gives somewhat higher energy flux values. Because the measured values of $\overline{u^2 u_3}$ are of the order of 10^{-4} to

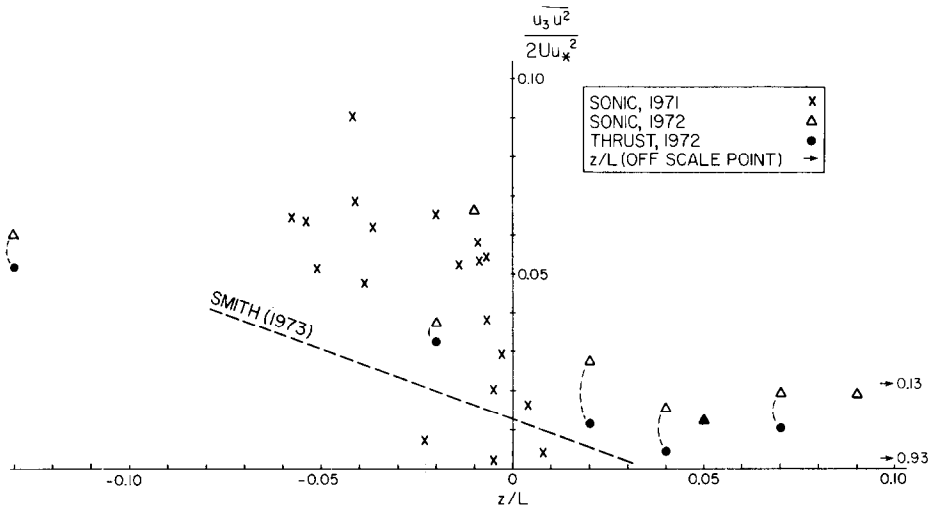

Fig. 10. Vertical kinetic energy flux as a function of stability. Dotted lines join simultaneous observations.

$10^{-5}\ U^3$, the energy-flux values are particularly sensitive to small anemometer errors, such as cross-coupling of the components or nonlinearity.

5. Conclusions

A thrust anemometer and a sonic anemometer give similar values of wind speed and drag coefficient when operated simultaneously on the same mast. The anemometers are shown to have equivalent performance within the resolution of this experiment, that is up to 3 Hz, by coherence and phase comparisons of the velocity components. The boundary-layer fluxes over Lake Ontario are found to be substantially the same as those already reported in the literature over other bodies of water at similar wind speeds and stabilities. For near-neutral stratification and at a wind speed of about 10 m s^{-1}, the eddy flux coefficients may be taken to be $C_{10}=C_T=C_Q=1.2\times10^{-3}$.

These coefficients may be used to compute stress, heat flux and evaporation budgets using mean wind, temperature and humidity measurements from an array of buoys covering Lake Ontario during IFYGL. As results from other boundary-layer studies become available, it may become possible to include variation of C_T with stability and of C_{10} with wind speed.

Acknowledgements

The author wishes to thank E. G. Banke for participation in the field trip and for operation of the sonic anemometer. Assistance by F. C. Elder and M. Donelan, and the use of field facilities established by CCIW staff are gratefully acknowledged. The data were analyzed by R. F. Brown of Metro Computer Applications. E. G. Banke, R. H. Loucks and F. W. Dobson made helpful comments on the manuscript.

References

Banke, E. G. and Smith, S. D.: 1973, 'Wind Stress on Arctic Sea Ice', *J. Geophys. Res.* **78** (in press).

Brocks, K. and Krügermeyer, L.: 1970, 'The Hydrodynamic Roughness of the Sea Surface', *Berichte des Instituts für Radiometereologie und Maritime Metereologie No. 14*, U. of Hamburg, 55 pp.

Hasse, L.: 1968, 'On the Determination of Vertical Transports of Momentum and Heat in the Atmospheric Boundary Layer at Sea' (in German), *Hamburger Geophysicalische Einzelschriften*, Heft 11, 70 pp.; English Translation, *Tech. Rep. 188*, Dept. of Oceanography, Oregon State U., 1970.

Kaimal, J. C.: 1968, 'The Effect of Vertical Line Averaging on the Spectra of Temperature and Heat Flux', *Quart. J. Roy. Metereol. Soc.* **94**, 149–155.

Kaimal, J. C., Wyngaard, J. C., and Haugen, D. A.: 1968, 'Deriving Power Spectra from a Three-Component Sonic Anemometer', *J. Appl. Meteorol.* **7**, 827–837.

Kaimal, J. C.: 1969, 'Measurement of Momentum and Heat Flux Variations in the Surface Boundary Layer', *Radio Sci.* **4**, 1147–1153.

McBean, G. A.: 1971, 'The Variations of the Statistics of Wind, Temperature and Humidity Fluctuations with Stability', *Boundary-Layer Meterol.* **1**, 438–457.

Miyake, M., Donelan, M., McBean, G., Paulson, C., Badgley, F., and Leavitt, E.: 1970, 'Comparison of Turbulent Fluxes over Water Determined by Profile and Eddy Correlation Techniques', *Quart. J. Roy. Meteorol. Soc.* **96**, 132–137.

Pond, S., Phelps, G. T., Paquin, J. E., McBean, G., and Stewart, R. W.: 1971, 'Measurements of Turbulent Fluxes of Momentum, Moisture, and Sensible Heat over the Ocean', *J. Atmospheric Sci.* **28**, 901–917.

Sheppard, P. A., Tribble, D. T., and Garratt, J. R.: 1972, 'Studies of Turbulence in the Surface Layer over Water (Lough Neagh). Part I. Instrumentation, Program, Profiles', *Quart. J. Roy. Meteorol. Soc.* **98**, 627–641.

Smith, S. D.: 1969, 'A Sensor System for Wind Stress Measurement', *Rep. 1969-4*, Bedford Institute of Oceanography, Dartmouth, N.S., 64 pp.

Smith, S. D.: 1970, 'Thrust-Anemometer Measurements of Wind Turbulence, Reynolds Stress, and Drag Coefficient over the Sea', *J. Geophys. Res.* **75**, 6758–6770.

Smith, S. D.: 1972, 'Wind Stress and Turbulence over a Flat Ice Floe', *J. Geophys. Res.* **77**, 3886–3901.

Smith, S. D.: 1973, 'Thrust Anemometer Measurements over the Sea Re-Examined', *Rep. BI-R-73-1*, Bedford Institute of Oceanography, Dartmouth, N.S., 23 pp.

Smith, S. D. and Brown, R. F.: 1971, 'Program A TO D for Analog-to-Digital Conversion of Time-Series Data', *Computer Note 1971-2-C*, Bedford Institute of Oceanography, Dartmouth, N.S., 51 pp.

Thorpe, M. R., Banke, E. G., and Smith, S. D.: 1973, 'Eddy Correlation Measurements of Evaporation and Sensible Heat Flux over Arctic Sea Ice', *J. Geophys. Res.* **78**, in press.

Wieringa, J.: 1973, 'Gust Factors over Open Water and Built-Up Country', *Boundary-Layer Meteorol.* **3**, 424–441.